Martinelli Roberto

Trajectories of cloud particles within exoplanet atmospheres

BACHELOR'S THESIS

to achieve the university degree of

Bachelor's degree programme: Physik

submitted to

Graz University of Technology

Supervisor

Prof. Dr.rer.nat. Christiane Helling,
Institut für Theoretische Physik - Computational Physics

Co-Supervisor

MSc. Sven Kiefer,
OEAW

Graz, March 2024

Abstract

Exoplanets orbit other stars than our Sun in extrasolar systems lightyears away from earth. Similair to planets in our solar system, exoplanets have different chemical compositions and can have an atmosphere. These chemically diverse atmospheres can also form clouds with a large variety in terms of cloud structure. Exoplanet atmospheres of planets that are tidally locked around their host star are great objects to study. For this simulation an exoplanet of the type Hot Jupiter with an effective temperature of $T_{eff} = 800K$ was modelled. In this thesis, trajectories of particles within an Hot Jupiter atmosphere were simulated using data of GCM simulations while considering changing size of the particles due to changes in the cloud particle properties inside the atmosphere. For different altitude layers in the atmosphere the motion equations for trajectories of cloud particles were solved in three dimensions. The trajectories for particles originating around the exoplanet inside the atmosphere were studied and interpreted in their behaviour. The results show that there are three well defined regions in terms of altitude, pessure and temperature inside the atmosphere. Particle tajectories are defined by the regions in the atmosphere where particles are either created ($> 5.000.000m$), evaporated ($< 3.500.000m$) or mostly reside in large clouds . A cloud dominated region of this exoplanet atmosphere was spotted between $3.500.000m$ and $4.500.000m$ altitude. In lower altitude layers possible low pressure areas with resulting strong updrafts, downward trajectories for evaporating particles and gyres were identified. Particle trajectories at high altitudes have a strong correlation to gas temperature distribution. This is caused by Rossby waves because of the rotation of the exoplanet featuring hot and cold spots in the atmosphere.

Contents

Chapter 1

Introduction

There are more than 5600 extrasolar planets known as of March 2024 (exoplanet.eu, 2024). Similair to our solar system there is a variety of planets in terms of composition, size and distance to their host star. Some planets consit of light elements such as hydrogen or helium others of water, rock or iron. In general for known mass and radius of an exoplanet, a mean density can be derived to classify the planet type as a gaseous-, terrestrial- or earth like planet.

In this thesis we model a Hot Jupiter, which is a type of gaseous exoplanets with similair mass to planet Jupiter in our solar system. The exoplanet is tidally locked, orbiting its host star very closely with a short orbiting period facing with the same side directly at the star.

1.1 Cloud formation

The atmosphere of an gaseous exoplanet can be chemically rich (e.g., CO, SiO, CaH, H_2O, TiO_2, $Mg(OH)_2$) (Helling, 2019). Gas temperature of the atmosphere of the simulated exoplanet ranges with effective temperature of $800K$ from about $< 500K$ at high altitudes to $> 2.500K$ at low altitudes. At high altitudes, cluster formation (e.g., $(TiO_2)_N$, $(SiO)_N$, $(V_2O_5)_N$) and nucleation by gas-gas reaction of said chemically rich gas takes place. This process creates cloud particles with increasing average size the lower in the atmosphere (higher gas temperature) the particle decends. Surrounding temperature, gas density and wind speed must be favourable in order for the particle to grow. At altitudes where the surrounding gas temperature is below sublimation temperature, bulk growth by gas-surface reactions further increases particle size. For different gas density and temperature, material composition of particles changes because of changing thermal stability. Maximum size for a particle is archieved when the rate of growth equals rate of evaporation to maintain thermal stability. At low altitudes where gas temperature is higher than sublimation temperature, decreasing thermal stability causes bulk evaporation. Average particle size decreases until complete evaporation of the material which replenishes the atmosphere. In conclusion particle size has its maximum where gas temperature is close to sublimation temperature and clouds are the most chemically rich.

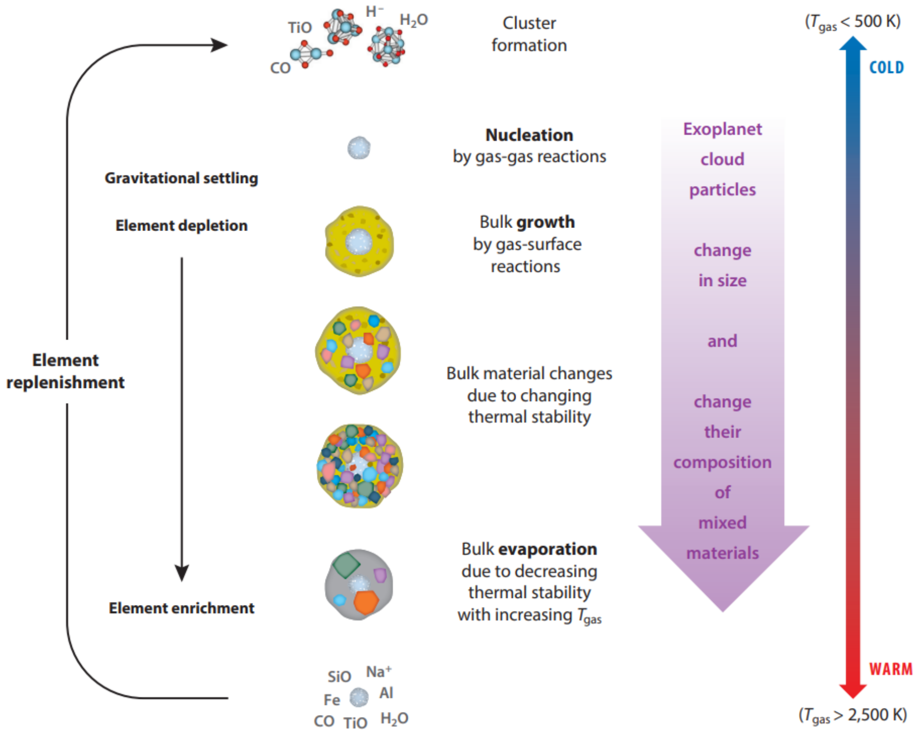

Figure 1.1: Cloud formation process, image taken from (Helling, 2019)

1.2 GCM

Similair to earth's atmosphere cloud formation and climate of an exoplanets atmosphere can be simulated using General Circulation Models (GCM). A GCM predicts a planets atmosphere over time by solving equations of hydrodynamics considering atmospheric motion and heat transfer. For MITgcm these equations are computed on a cubed-sphere grid which divides the atmosphere into unit cells.

Applying GCMs to Hot Jupiters result in a fast equatorial jet stream, advecting air and therefore heat in an eastward direction (Baeyens et al., 2021). This causes the hottest regions to be displayed eastward from the substellar point by tens of degrees longitude. The equatorial jet results from interaction with standing Rossby waves induced by the day-night thermal forcing. These waves are formed due to strong variations in radiative heating, namely intense dayside heating and nightside cooling (Showman and Polvani, 2011). Rossby waves are a consequence of the coriolis effect caused by rotation of the planet.

1.3 Motion Equation

In order to take the changing size of the cloud particle into account, drift velocity is also considered due to dust growth and evaporation. Drift velocity is also important for the frictional force in the next section which depends on this relative velocity between the dust particle and the surrounding gas (Woitke, P. and Helling, Ch., 2003).

To formulate the equation of motion for a spherical cloud particle which is similar for a dust particle in a brown dwarf, the approach of (Woitke, P. and Helling, Ch., 2003) can be used. To derive the terminal drift velocity of a dust particle, they used the following equation:

$$m_d \vec{x''} = \vec{F}_{grav}(\vec{x}, r) + \vec{F}_{radi}(\vec{x}, r) + \vec{F}_{fric}(\vec{x}, r, \vec{v}_{drift}) \tag{1.1}$$

with the particles mass:

$$m_d = \frac{4\pi}{3} r^3 \rho_d \tag{1.2}$$

where $\vec{x}$ corresponds to the position of the particle, $r[cm]$ is its radius, $\rho_d[\frac{g}{cm^{-3}}]$ the density of a certain spherical size and $\vec{v}_{drift}[\frac{cm}{s}]$ the drift velocity. $\vec{F}_{grav}[dyn]$ is the gravitational force, $\vec{F}_{radi}[dyn]$ (radiative force) takes radiative effects due to absorption and scattering of photons into account and $\vec{F}_{fric}[dyn]$ (frictional force) is excerted by surrounding gas collisions as frictional force. Since the radiative force is small and scales for large grains as a^2 (particle size), it can be shown Woitke, P. and Helling, Ch. (2003), that this force contribution is much smaller than the gravitational part for brown dwarfs, or exoplanets, simplifies the equation to:

$$\vec{F}_{grav}(\vec{x}, r) >> \vec{F}_{radi}(\vec{x}, r) \tag{1.3}$$

$$m_d \vec{g}(x) + \vec{F}_{fric}(\vec{x}, r, \vec{v}_{eq.drift}) = 0 \tag{1.4}$$

This equation is valid for said *force equilibrium*. However, because of accreation of molecules $\frac{dr}{dt} \neq 0$ and non constant pressure of the surrounding gas $\frac{dp}{dt} \neq 0$, force equilibrium can only be reached locally. The concept of equilibrium drift is good enough for an approximation since a dust particle reaches its equilibrium driftvelocity much faster than hydrodnamical changes occur in the atmosphere. Another important note is that the driftvelocity is centered at the center of gravity of the planet.

1.4 Motivation

The goal of this thesis is to study and interpret the behaviour of cloud particle trajectories in three dimensions while also considering the relative drift velocity. Previous work focussed mainly on the one dimensional case studying particle trajectories in vertical axis in terms of vertical movement and particle growth and evaporation.

The resulting simulation of three dimensional trajectories allows for imaging of cloud structures and significant patterns covering the whole atmosphere of the exoplanet. Influence of wind jets on particle trajectories at different altitudes can be considered as well as gyres or laminar trajectories in particular. The idea is to get a better understanding cloud particle movement in three dimensions.

Chapter 2

Methods

2.1 Dataset

In order to simulate the particle trajectories and solve their equation of motion for every timestep, two datasets were interpolated. This data containing gas temperature, wind velocities as well as drift velocity in the exoplanets atmosphere were taken from Baeyens et al. (2021) and Helling, Christiane et al. (2023):

- gas temperature and wind velocity profiles: $T[K]$, $v_x[\frac{cm}{s}]$, $v_y[\frac{cm}{s}]$, $v_z[\frac{cm}{s}]$ for every longitude, latitude, pressure/height coordinate (Baeyens et al., 2021)
- cloud profiles: $a[cm^3]$, $v_{dr}[\frac{cm}{s}]$ for every longitude, latitude, pressure/height coordinate (Helling, Christiane et al., 2023)

Interpolation was necessary due to different resolution of datapoints of the two datasets. The resulting interpolated dataset contained temperature, dust particle size and velocity in cartesian coordinates for every position of the datagrid. The longitudinal wind velocity, temperature and average dust particle size of the exoplanets atmosphere is shown in figures 2.1 to 2.3.

Figure 2.1 (i) shows that drift velocity discussed in section 1.3 is orientated in the negative z-direction. Longitudinal wind velocity v_x is defined in the longitude-latitude plane with positive values in direction of positive longitude. In subfigure (ii) of figure 2.1 longitudinal wind velocities are plotted which already shows strong equatorial wind jets at the upper half of the atmosphere:

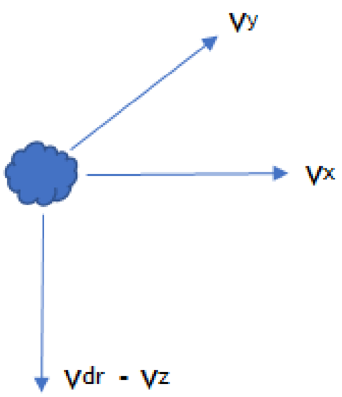

(i) Dust particle velocities

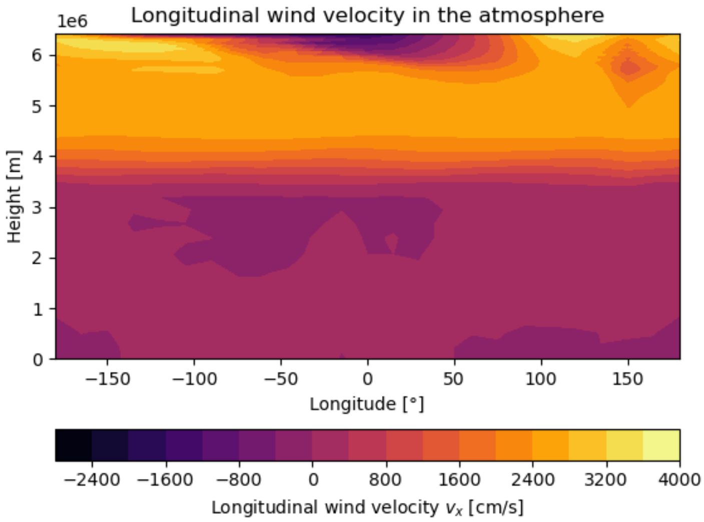

(ii) Longitudinal wind jets in the atmosphere

Figure 2.1: Wind velocities affecting the particle and plot of the longitudinal component

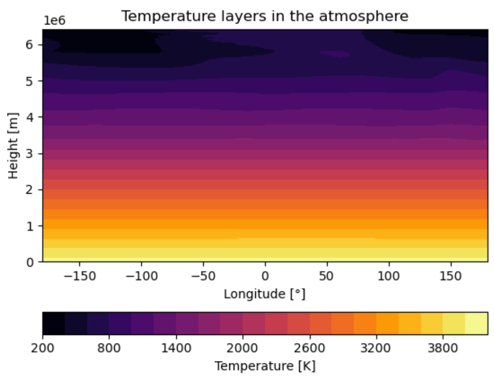

(i) Temperature plot

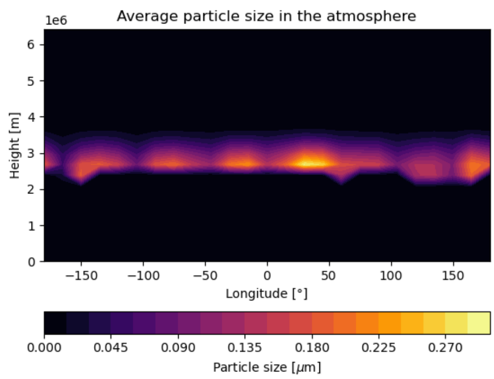

(ii) Dust particle size

Figure 2.2: Temperature and dust particle size for the Hot Jupiter with $T_{eff} = 800K$

In figure 2.2 on the left side (i), we observe an increase of gas temperature for decreasing altitude in the atmosphere. The other picture (ii) shows average dust particle size $a[\mu m]$ for every height in the dataset over the longitudes covering the entire atmosphere. We already locate the estimated region for larger clouds due to larger average particle sizes between 2.500.000m and 3.000.000m in altitude.

Furthermore, gas temperature at high altitudes in the atmosphere features hot and cold spots as shown in figure 2.3 below:

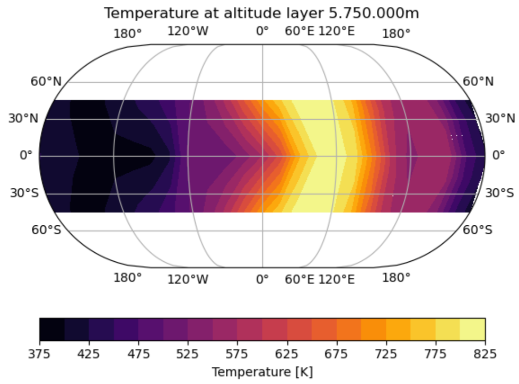

(i) Altitude layer 5.750.000m

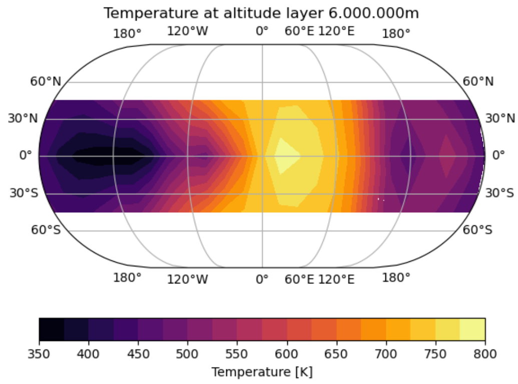

(ii) Altitude layer 6.000.000m

Figure 2.3: Temperature hot and cold spots at high altitudes

The final datagrid ranges from -180° to 180° in longitude around the sphere but only between 0° and 45° in latitude due to limited data. However, since the rotational axis of the planet and the orbit are aligned, the data was mirrored for the lower hemisphere of the exoplanet.

Tidally locked Hot Jupiters with intermediate effective temperatures are a very good astronomical object to study in terms of trajectories inside the atmosphere. Effective temperature of an object is defined by the temperature of a Black Body of the same size that would radiate the same total amount of electromagnetic power as emitted by the object. They provide continuous cloud coverage which is essential to this project (Helling, Christiane et al., 2023). Cool planets with homogenous cloud coverage or ultra-hot planets with no clouds at all would not provide interesting trajectories to study.

2.2 Mathematical approach

It is important to note that while the velocities of the dataset are given in cartesian coordinates, we want to present the trajectories in spherical coordinates. Therefore a routine to transform the local coordinates (velocities) from cartesian to spherical and back from spherical to cartesian is needed. The differential equations describing the motion of the particle were solved for every iteration in cartesian coordinates using Explicit Euler method, to avoid transformation of the velocities:

$$\vec{v}(v_x, v_y, v_z, v_{drift}) = \frac{d\vec{x}}{dt} \tag{2.1}$$

For every calculation, the altitude coordinate points in z-direction and due to the difference in position between iterations being very small compared to the size of the planet, parallel plane assumption is valid. The result was a correctly rotated coordinate system for which the trajectories of the cloud particles could be plotted. Since we defined the drift velocity to be in the direction of the center of gravity of the exoplanet, we transform the coordinates as follows:

$$cos(\phi) = \frac{\widetilde{r}}{r} \tag{2.2}$$

$$\Delta x = \Delta\phi \frac{2\pi\widetilde{r}}{360} = \Delta\phi \frac{\pi cos(\theta) r}{180} \tag{2.3}$$

$$\Delta y = \Delta\theta \frac{2\pi r}{360} = \Delta\theta \frac{\pi r}{180} \tag{2.4}$$

Figure 2.4 shows how the radius $r[\mu m]$ is reduced $\widetilde{r}$ at the surface of the exoplanet for higher altitudes. Due to the reduced radius the cartesian coordinates in xy-plane are also transformed with polar angle θ [°] and azimuthal angle ϕ [°] considering rotation of the coordinate system to the center of gravity for every iteration of the trajectory.

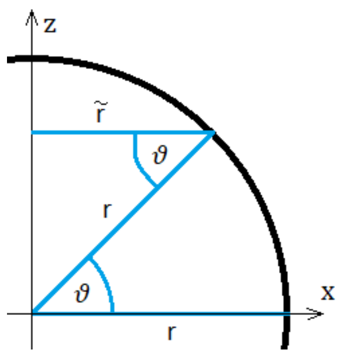

Figure 2.4: Radius $\widetilde{r}$ for latitude $\theta \neq 0$

To present the trajectories in three dimensions, altitude layers of the atmosphere were sliced from $500.000m$ to $6.000.000m$ in steps of $500.000m$. For every fixed layer of the exoplanet with $T_{eff} = 800K$, 49 trajectories were plotted evenly distributed in terms of initial longitude and latitude to cover the whole spherical atmosphere.

Chapter 3

Results

As stated in section 2 the plots display fixed initial starting height of the 49 dust particle trajectories for one altitude layer viewed from *above*. Alongside this plot we also study the longitude over change in height for the same trajectories. Particle trajectories were simulated between ± 45° latitude in 15° steps and in evenly spaced starting longitudes: -150° (blue), -100° (green), -50° (red), 0° (black), 50° (cyan), 100° (magenta) and 150° (yellow).

3.1 Low altitudes

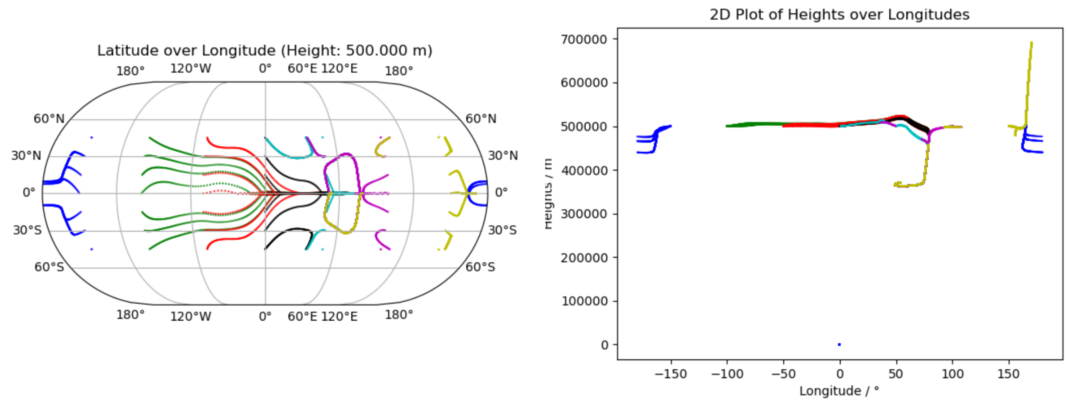

Figure 3.1: Trajectories at initial height 500.000m

Figure 3.1 shows particle trajectories with an initial height of 500.000m. Most of the particles move in the same direction as the rotational direction of the exoplanet.

However, the blue trajectories starting at -150° longitude move the other way around the planet. This trajectory orientation against the planets rotation is because of the negative longitudinal wind velocity in figure 2.1 (ii) for that longitude. Same for trajectories originating from longitude 100° (magenta), 150° (yellow) and some of 50° (cyan).

3.2 Downward trajectory

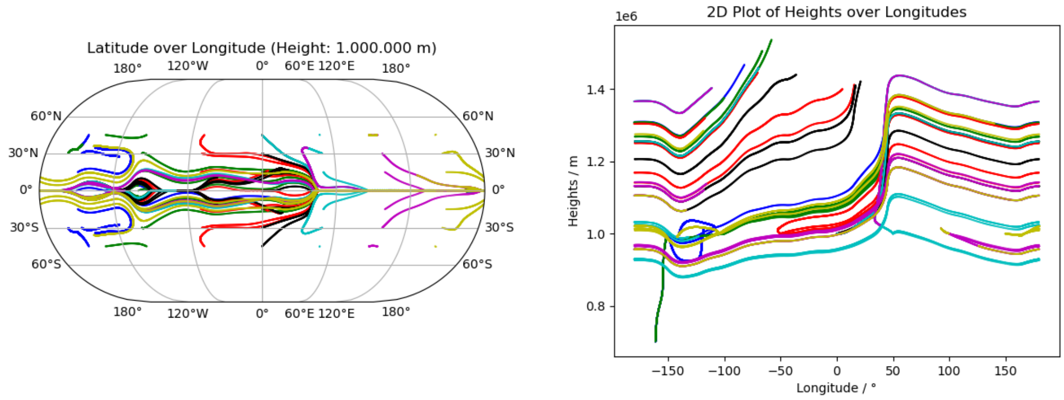

Figure 3.2: Laminar trajectories and downwards trajectory at 1.000.000m

For particle trajectories originating at 1.000.000m altitude, on the left hemisphere along the equator, trajectories tend to be more laminar which is also visible at the heights plot. A massive updraft near the substellar point at about 30° longitude causes the particles to ascend but at different heights. There is also one interesting trajectory (starting at -100°, green) going downwards at about -150° in altitude. In general trajectories sustain much longer in the atmosphere when directly compaired to figure 3.1.

3.3 Updrafts below cloud region

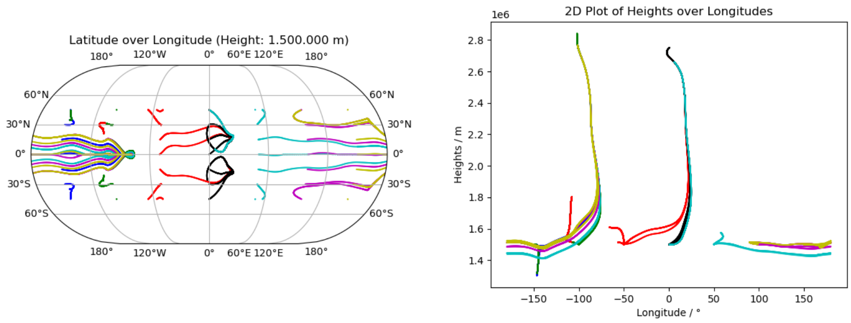

Figure 3.3: Updraft trajectories at initial height 1.500.000m

Trajectories originating at altitude layer of 1.500.000m and above receive a massive updraft at about -90° and 10° longitude. Another obervation in the last two figures is that trajectories are longer since the particles are able to move further in the atmosphere due to faster particles.

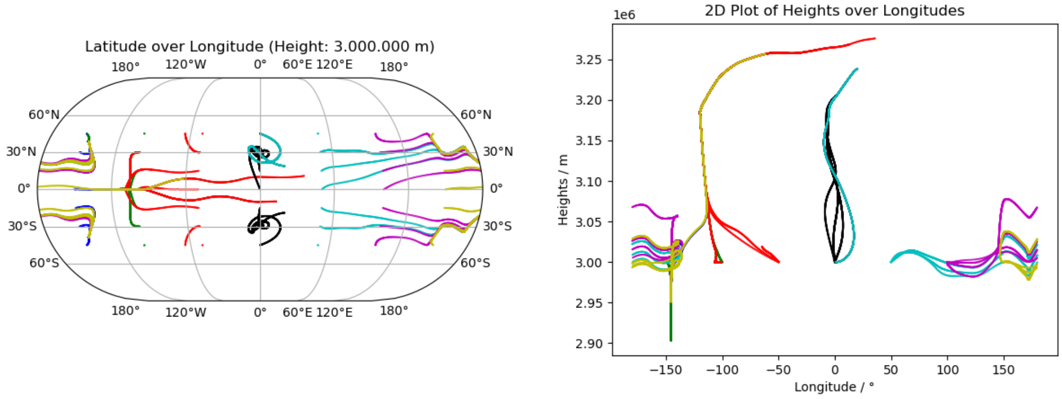

Figure 3.4: End of updraft trajectories at initial height 3.000.000m

The updraft trajectories stop their ascend asymptotically for trajectories starting at 3.000.000m altitude, indicating a region of strong equatorial wind jets (red trajectory). Near 0° longitude trajectories (black) follow a spiral shape as shown in the surface plot on the left.

3.4 Cloud layer

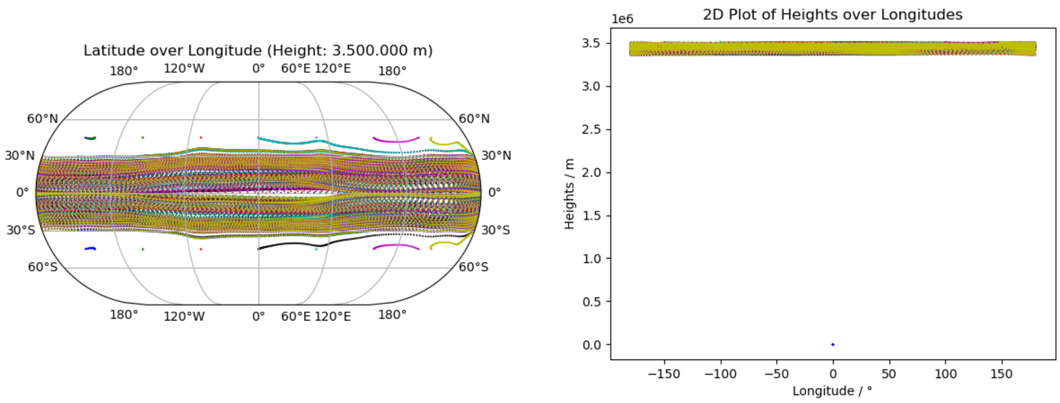

Figure 3.5: Cloud layer at initial height 3.500.000m

At 3.500.000m altitude particles reside in the cloud layer, indicated by very strong wind jets (trajectories are dotted due to covering more distance in the same time). There is almost no change in height of the trajectories since the particles can not escape from that layer.

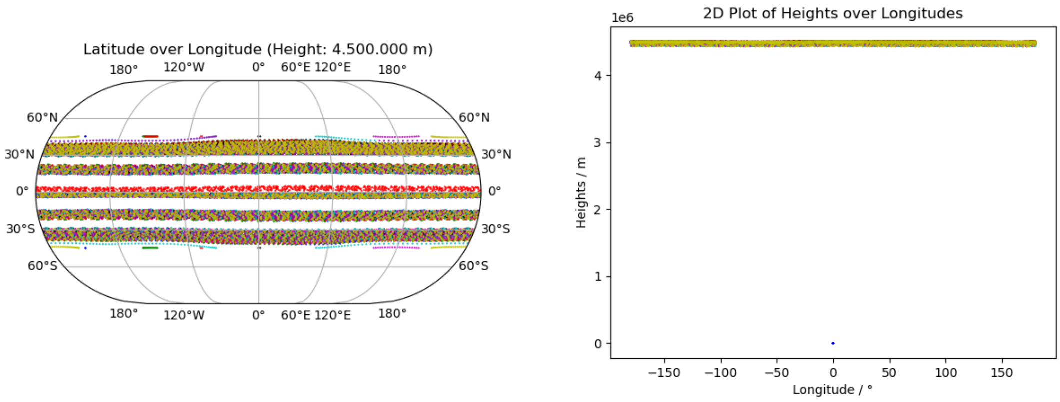

Figure 3.6: Thinner cloud layer at initial height 4.500.000m

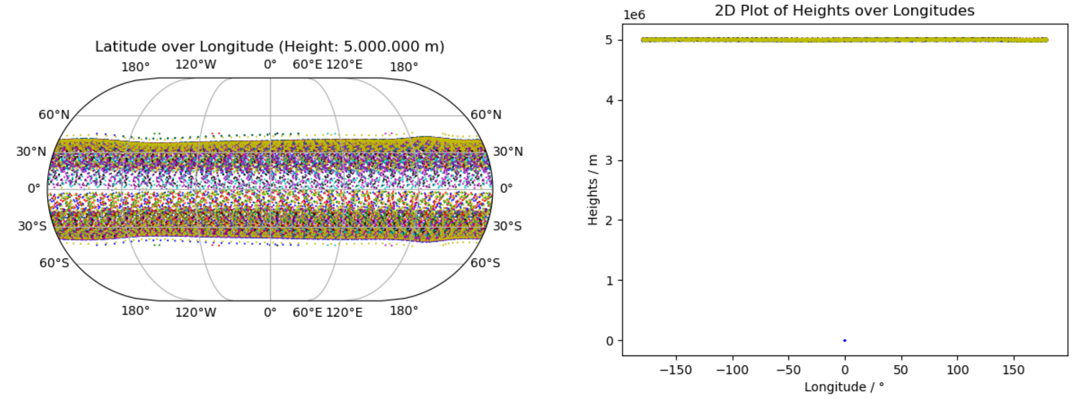

Figure 3.7: Cloud layer with faster particles 5.000.000m

Higher altitudes (4.500.000m to 5.000.000m) show that clouds get thinner, but particles move faster comparing to lower altitudes. Another observation is that for every plot in the cloud layer, the clouds get thinner in terms of total height as particles size gets smaller in the atmosphere.

3.5 High altitudes

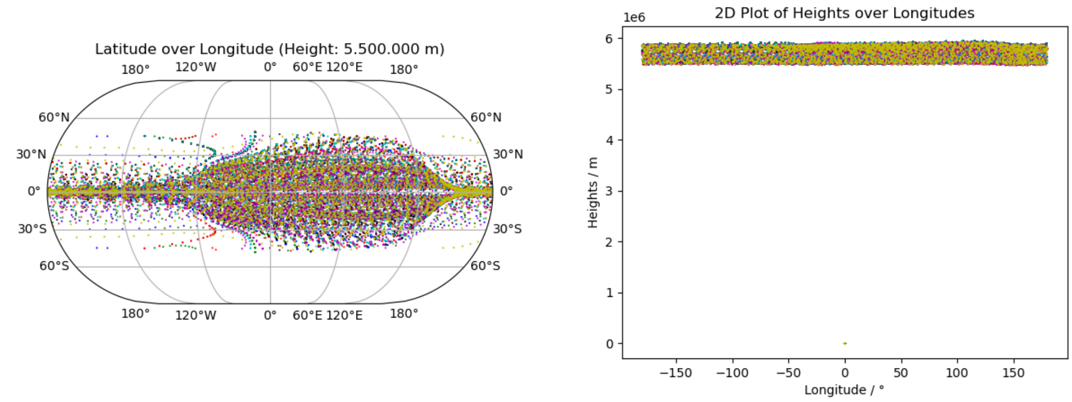

Figure 3.8: End of cloud layer at initial height 5.500.000m

Particle trajectories at altitudes high above cloud layer as seen in figure 3.8 have one rather large distinctive spot eastern to the substellar point round 60° longitude where a large amount of particles reside at high velocities. At the end of the simulated altitude range in figure 3.9, we observe two circular trajectories located around -170° longitude:

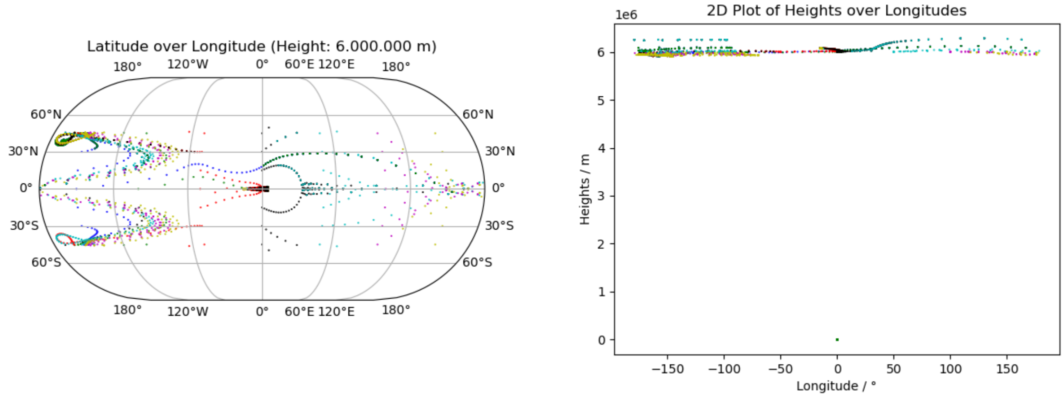

Figure 3.9: Above cloud layer at initial height 6.000.000m

Chapter 4

Discussion

In the following sections the atmosphere layers of the results in chapter 3 are discussed to analyse the trajectories and patterns found. The sections follow the same order as in chapter 3.

4.1 Low altitudes

In general for trajectories outside latitude values $\pm$ 45° there is no data to calculate the motion. Either the trajectory stops at that latitude or only a single dot is plotted. Dotted lines of the scatter plots are an indicator for faster particle velocities due to stronger winds. For such trajectories the particle covers more distance in the same amount of time.

For low altitudes there are only short and distinguishable trajectories visible due to evaporation and decreasing size of the particles at high gas temperatures. Furthermore, as seen in figure 2.1 (ii), wind velocities are low at that altitude layers in the atmosphere. The blue trajectory moves against the exoplanets rotational direction since longitudinal wind velocity is negative in that region. This motion could also be explained by an updraft wind at 160° longitude that spirals the particle in the other direction.

4.2 Downward trajectory

The increase in trajectories alongside each other indicates that particle remain much longer in that atmospheric layer than in section 3.1. As stated in (Rauscher and Menou, 2010) about vertical wind structure, for trajectories moving from higher altitudes to this layer of the atmosphere, the main driver is momentum transport.

Particle Trajectories in the lower levels have no stationary state which is the reason for vertical wind structure at this altitudes. It is also visible in figure 3.2 that wind jets near the equator are much stronger and decrease with distance. The mentioned downwards trajectory with green colour visible in the heights over longitude plot at -150° longitude shows fast evaporation as the particle decends quickly in the atmosphere and decreases in size. This result is also given by the data of average particle size in figure 2.2 (ii). In figure 4.1 below only the trajectories nearby are plotted for better visibility:

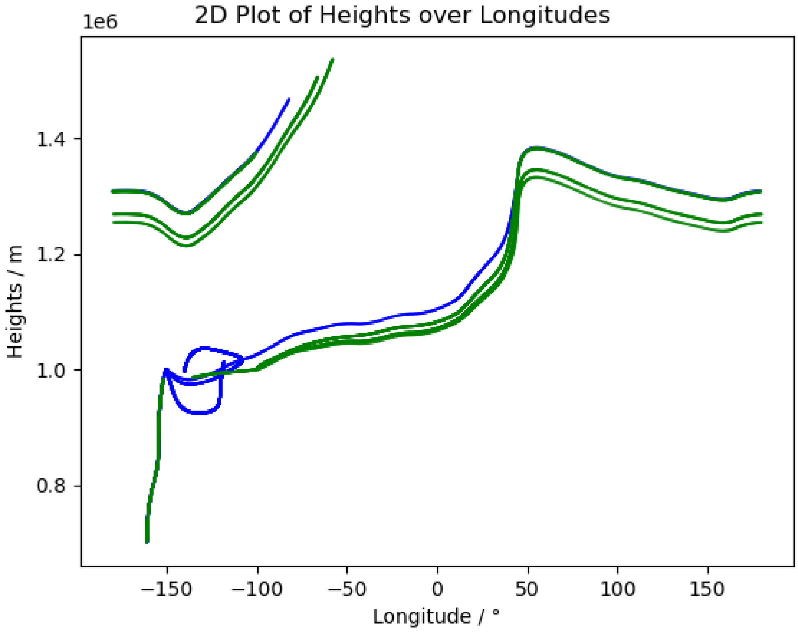

Figure 4.1: downwards trajectories starting at longitude -150° (blue) and -100° (green)

4.3 Updrafts below cloud region

Updrafts highlighted in section 3.3 can be explained with a low pressure areas that cause the particles to ascend at that longitudes. This idea is supported by the black spiral trajectory shown in figure 3.5. The red asymptotical trajectory at 3.500.000m is a strong indicator for a strong equatorial wind jets reaching cloud layer. Cloud Particles moving upward because of the low pressure area reach the lower end of the cloud layers with much faster equatorial wind jets resulting in very small change of altitude for that trajectory after reaching that layer asymptotically.

4.4 Cloud layer

Particles reach their maximum size due to bulk growth possibly at a height of 3.500.000m. Trajectories cover the most area in the latitude-longitude plane as shown in figure 3.6. According to figure 2.2 (ii), we would expect that to be lower in the atmosphere comparing with the plot of average particle size.

Figures 3.7 and 3.8 show gaps in the latitude-longitude plane of the trajectories which are caused by smaller wind velocities in latitude direction. Once again, if we compare with the data in figure 2.1 (longitudinal wind velocity and temperature), cloud thickness changes due to different properties in this layers of the atmosphere. Especially the change to very fast wind velocities is significant and causes the trajectories to spread from each other resulting in a *thinner* cloud. Looking at only temperature distribution, very similar results have been found for exoplanet HD 209458b (Cooper and Showman, 2005), where the results show a stable superrotating jet at the equator as well as little longitudinal variability for the temperature structure at this layer.

4.5 High altitudes

For the highest observed altitudes where temperature in the atmosphere is below sublimation temperature, creation of dust grains in form of nucleation takes place. Furthermore in these figures trajectories of particles are very similair to temperature distribution in high and low temperature areas. They display a large tidally locked temperature hot spot (figure 3.8) facing the host star which is not directly centered in terms of longitude due to the rotation of the exoplanet as well as two mirrored Nightside gyres around the equator at about -170° longitude (figure 3.9). These hot and cold spots are caused by cone like equatorial wind jets in the exoplanets atmosphere at that height range. Particles at these altitudes are very fast in terms of longitudinal wind velocity while many of them end up in that gyres of the cold spots. The temperature profiles for high altitudes displayed at figure 2.3 feature this hot and cold spots for altitudes 5.750.000m and 6.000.000m. Due to the given dataset and interpolation the temperature resolution in these figures is limited.

Chapter 5

Conclusion

In this thesis, trajectories of dust particles within an exoplanets atmosphere of the type tidally locked Hot Jupiter with an effective temperature of $800K$ were modelled. Using a GCM simulation (Baeyens et al., 2021) and a dataset with cloud properties of the atmosphere (Helling, Christiane et al., 2023), the positions and trajectories of cloud particles were calculated for different altitude layers in the atmosphere. For a particle with variying size due to evaporation and condensation depending on the inital height of its trajectory, three different regions in this simulation could be established:

- At low altitudes in the atmopshere (below $3.000.000m$) most particles slowly evaporate and therefore decrease in size. This happens due to surrounding gas tempereatures being higher than sublimation temperature. This region features particle trajectories with significant changes in altitude. Downward trajectories and strong updrafts due to possible low pressure areas could be shown. Altitudes just below cloud layer where most of the particles with larger average size reside, feature trajectories that point asymptotically parallel to the equator of the exoplanet.
- Dust particles residing at altitudes ($3.500.000m$ to $4.500.000m$), where gas temperature is near sublimation temperature, have the largest average dust grain size. Trajectories of particles in that region have almost no increase or decrease in height due to strong equatorial wind jets. Trajectory density inside these clouds decreases for higher altitudes. However, results show faster particle velocities at higher atmosphere layers.
- Above the cloud layers ($> 5.000.000m$) at low temperatures below sublimation temperature, nucleation creates particles and the trajectories are very similair to the temperature distribution of the exoplanets atmopshere at that altitude

showing distinguishable hot and cold spots.

5.1 Outlook

In the future Hot Jupters with higher effective temperatures could be studied in terms of their particle trajectories since temperature is such an important factor in the process of dust growth and evaporation in this simulation. Planets with other effective temperatures might change how these three regions of particle evaporation and condensation as well as cloud layers are distributed inside the atmosphere. Especially average particle size of said planets with higher effective temperature might change significantly.

Trajectories near the poles of an exoplanets atmosphere might also be interesting due to possible different behaviour at greater latitudes which are not included in this thesis. Trajectories further away from the equator would behave much different to the discussed results due to different wind velocities.

Bibliography

R. Baeyens, L. Decin, L. Carone, O. Venot, M. Agúndez, and P. Mollière. Grid of pseudo-2D chemistry models for tidally locked exoplanets - I. The role of vertical and horizontal mixing. *MNRAS*, 505(4):5603–5653, Aug. 2021. doi: 10.1093/mnras/stab1310.

C. S. Cooper and A. P. Showman. Dynamic meteorology at the photosphere of hd 209458b. *The Astrophysical Journal*, 629(1):L45, jul 2005. doi: 10.1086/444354. URL `https://dx.doi.org/10.1086/444354`.

exoplanet.eu. Encyclopedia of exoplanetary systems, 2024. URL `https://exoplanet.eu`. Accessed on March 2, 2024.

C. Helling. Exoplanet clouds. *Annual Review of Earth and Planetary Sciences*, 47(1):583–606, 2019. doi: 10.1146/annurev-earth-053018-060401. URL `https://doi.org/10.1146/annurev-earth-053018-060401`.

Helling, Christiane, Samra, Dominic, Lewis, David, Calder, Robb, Hirst, Georgina, Woitke, Peter, Baeyens, Robin, Carone, Ludmila, Herbort, Oliver, and Chubb, Katy L. Exoplanet weather and climate regimes with clouds and thermal ionospheres - a model grid study in support of large-scale observational campaigns. *Astronomy and Astrophysics*, 671:A122, 2023. doi: 10.1051/0004-6361/202243956. URL `https://doi.org/10.1051/0004-6361/202243956`.

E. Rauscher and K. Menou. Three-dimensional modeling of hot jupiter atmospheric flows. *The Astrophysical Journal*, 714(2):1334, apr 2010. doi: 10.1088/0004-637X/714/2/1334. URL `https://dx.doi.org/10.1088/0004-637X/714/2/1334`.

A. P. Showman and L. M. Polvani. Equatorial superrotation on tidally locked exoplanets. *The Astrophysical Journal*, 738(1):71, aug 2011. doi: 10.1088/0004-637X/738/1/71. URL `https://dx.doi.org/10.1088/0004-637X/738/1/71`.

Woitke, P. and Helling, Ch. Dust in brown dwarfs - ii. the coupled problem of dust formation and sedimentation. *Astronomy and Astrophysics*, 399(1):297–313,

2003. doi: {10.1051/0004-6361:20021734}. URL https://doi.org/10.1051/0004-6361:20021734.

Appendix

The following figures show particle trajectories of altitude layers that were not discussed due to already present features of altitude layers in section 3.

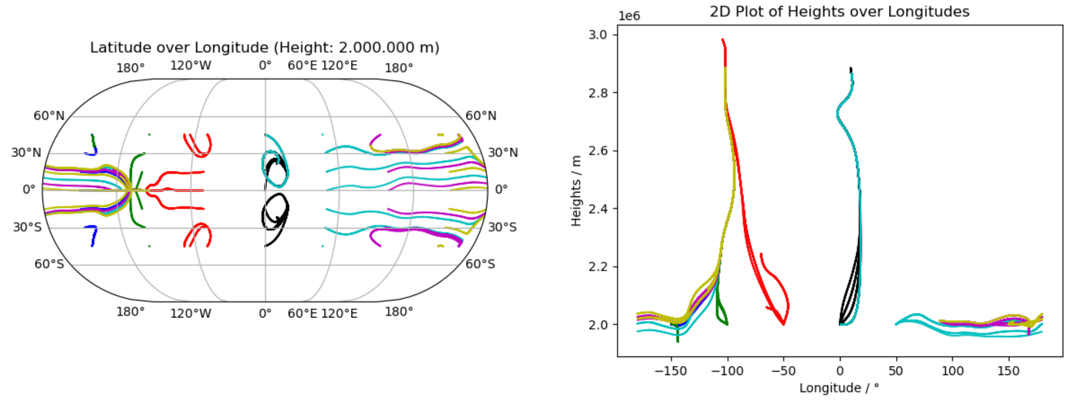

Figure 5.1: Particle trajectories at initial height 2.000.000m

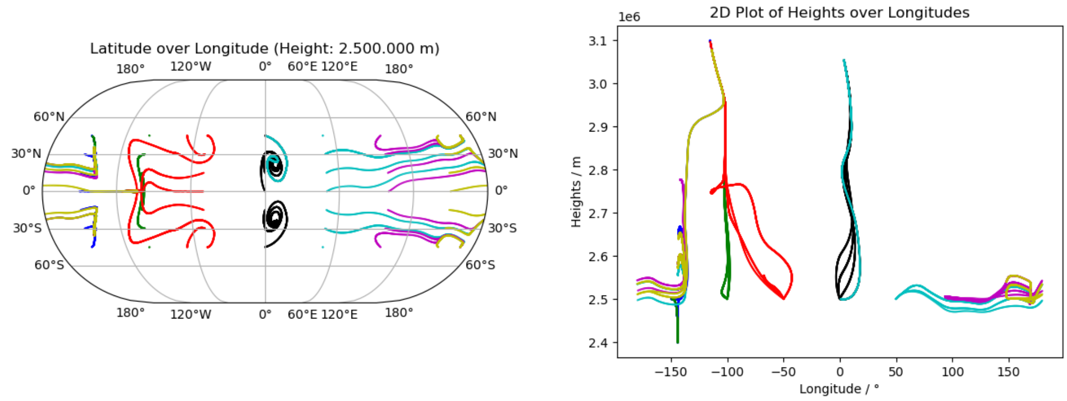

Figure 5.2: Particle trajectories at initial height 2.500.000m

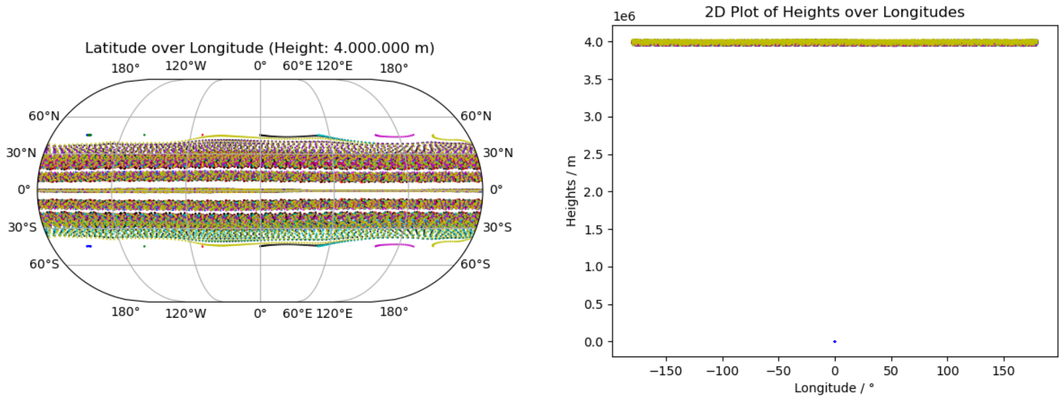

Figure 5.3: Particle trajectories at initial height 4.000.000m

Declaration

I declare that I have authored this thesis independently, that I have not used other than the declared sources/resources, and that I have explicitly indicated all material which has been quoted either literally or by content from the sources used. The text document uploaded to UNIGRAZonline or TUGRAZonline is identical to the present bachelor's thesis.

Graz, April 5, 2024